LETTER

https://doi.org/10.1038/s41586-019-1134-2

Molybdenum-catalysed ammonia production with samarium diiodide and alcohols or water

Yuya Ashida[1], Kazuya Arashiba[1], Kazunari Nakajima[2] & Yoshiaki Nishibayashi[1]*

The production of ammonia from nitrogen gas is one of the most important industrial processes, owing to the use of ammonia as a raw material for nitrogen fertilizers. Currently, the main method of ammonia production is the Haber–Bosch process, which operates under very high temperatures and pressures and is therefore very energy-intensive[1]. The transition-metal-catalysed reduction of nitrogen gas[2–6] is an alternative method for the formation of ammonia. In these reaction systems, metallocenes or potassium graphite are typically used as the reducing reagent, and conjugate acids of pyridines or related compounds are used as a proton source. To develop a next-generation nitrogen-fixation system, these reagents should be low cost, readily available and environmentally friendly. Here we show that the combination of samarium(II) diiodide (SmI_2) with alcohols or water enables the fixation of nitrogen to be catalysed by molybdenum complexes under ambient conditions. Up to 4,350 equivalents of ammonia can be produced (based on the molybdenum catalyst), with a turnover frequency of around 117 per minute. The amount of ammonia produced and its rate of formation are one and two orders of magnitude larger, respectively, than those achieved in artificial reaction systems reported so far, and the formation rate approaches that observed with nitrogenase enzymes. The high reactivity is achieved by a proton-coupled electron-transfer process that is enabled by weakening of the O–H bonds of alcohols and water coordinated to SmI_2. Although the current reaction is not suitable for use on an industrial scale, this work demonstrates an opportunity for further research into catalytic nitrogen fixation.

In recent years, transition-metal dinitrogen complexes have been found to be effective catalysts for the formation of ammonia under mild reaction conditions[2–6]. Our group has reported molybdenum iodide complexes that bear a pyridine-based PNP-pincer ligand [MoI_3(PNP)] (**1a**; PNP = 2,6-bis(di-*tert*-butylphosphinomethyl)pyridine) and catalyse the production of ammonia under ambient conditions, in which decamethylcobaltocene ($CoCp^*_2$) ($Cp^* = \eta^5\text{-}C_5Me_5$) and 2,4,6-trimethylpyridinium trifluoromethanesulfonate ([ColH]OTf) are used as a reducing reagent and a proton source, respectively[7]. Hereafter, we define this system as reaction system A (Fig. 1a). However, so far, the catalytic reductions of nitrogen gas to ammonia using transition-metal dinitrogen complexes have required reducing reagents and proton sources that are expensive and not readily available[2–7]. Simple alcohols and water are considered to be good candidates for proton sources. However, the use of these compounds as proton sources is difficult because they can react with low-valent transition metal complexes to give oxygen-coordinated complexes—for example metal–oxo and related complexes[8]—which generally inhibit the regeneration of the corresponding catalytically active metal dinitrogen complexes[9]. Although water and some simple alcohols have previously been used as proton sources in the formation of ammonia under mild conditions, these reactions were stoichiometric[9,10]; to our knowledge, their successful use in the catalytic formation of ammonia under mild conditions has not yet been reported[11,12].

To overcome this difficulty, we considered the combination of samarium(II) diiodide (SmI_2) and simple alcohols or water as the reducing reagent and proton source, respectively. SmI_2 is well established as an effective reducing reagent of various functional groups in organic reactions[13,14]. As a result, we have found a highly efficient method that can catalytically form ammonia from nitrogen gas using the combination of SmI_2 and ethylene glycol or water in the presence of molybdenum complexes as catalysts. In this reaction system, a stoichiometric amount of SmI_2 as a reducing reagent is required for the reduction of nitrogen gas to ammonia. Hereafter, we have defined the combination of SmI_2 and alcohols or water as reaction system B (Fig. 1a).

We reacted nitrogen gas at atmospheric pressure with 180 equivalents (equiv.) (to molybdenum catalyst **1a**) of SmI_2 as a reducing reagent and 180 equiv. (to **1a**) of ethylene glycol as a proton source, in the presence of **1a**, in tetrahydrofuran (THF) at room temperature for 0.5 h. This gave 39.7 equiv. of ammonia based on the molybdenum atom (65% yield based on SmI_2) together with 15.0 equiv. of hydrogen gas based on the molybdenum atom (16% yield based on SmI_2) (Fig. 1b). Separately, we confirmed that there was no formation of ammonia in the absence of either molybdenum complexes or nitrogen gas. Although the use of a longer reaction time (18 h) did slightly increase the yield of ammonia (up to 42.8 equiv. based on the Mo atom), 21.7 equiv. of ammonia were produced in just the first minute of the reaction. The time profile of the catalytic reaction is shown in Fig. 1c, in which it can be seen that ammonia formation is almost complete in 0.5 h. The turnover frequency (TOF) of ammonia formation—which is determined as the number of moles ammonia produced per molybdenum atom in the initial 1 min—is 21.7 min^{-1} (1,300 h^{-1}). This is nearly two orders of magnitude larger than that observed[7] in reaction system A (TOF = 28 h^{-1}).

Next, because the reducing ability of SmI_2 depends on the nature of the alcohol[15], we investigated these catalytic reactions using other alcohols as proton sources. For comparison, all catalytic reactions were carried out for 18 h. Typical results are shown in Table 1. When methanol (MeOH), ethanol (EtOH), 2-propanol (^{i}PrOH), *tert*-butyl alcohol (^{t}BuOH), 2,2,2-trifluoroethanol (CF_3CH_2OH) and phenol (PhOH) were used as proton sources instead of ethylene glycol, the amount of ammonia produced—based on the molybdenum atom of the catalyst—was smaller (Table 1, entries 1–7). [ColH]OTf was not an effective proton source in this reaction (Table 1, entry 8), although we had previously found that this triflate was the most effective proton source for ammonia formation in combination with $CoCp^*_2$ as a reducing reagent[7]. Conversely, no ammonia formation was observed at all when $CoCp^*_2$ was used as a reducing reagent in place of SmI_2 (Table 1, entry 9), although $CoCp^*_2$ (E_{red} in acetonitrile = −1.85 V versus the ferrocene/ferrocenium ion redox couple (Fc/Fc^+)[16]) has a higher reducing ability than SmI_2 (E_{red} in MeCN = −1.22 V versus Fc/Fc^+[17]). These results clearly indicate that the combination of SmI_2 and ethylene glycol—that is, reaction system B—is an effective reaction system for the formation of ammonia.

---

[1]Department of Systems Innovation, School of Engineering, The University of Tokyo, Tokyo, Japan. [2]Frontier Research Center for Energy and Resources, School of Engineering, The University of Tokyo, Tokyo, Japan. *e-mail: ynishiba@sys.t.u-tokyo.ac.jp

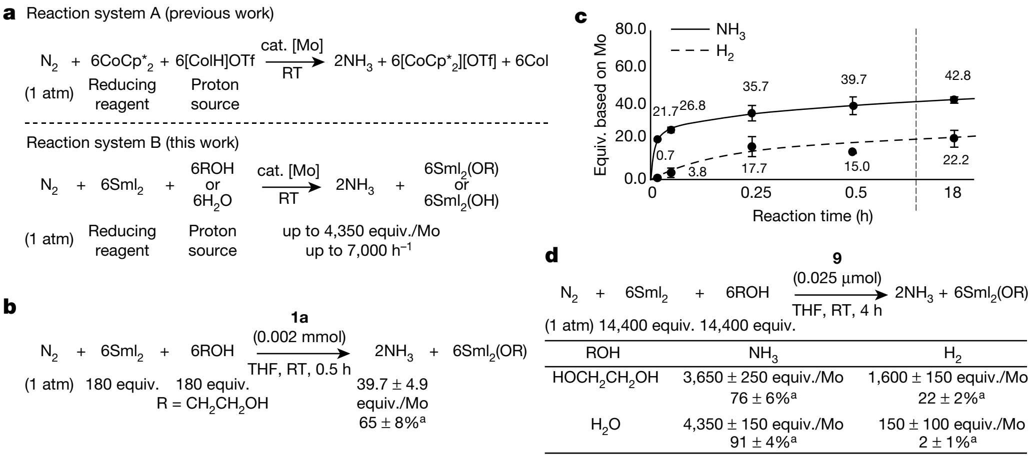

Fig. 1 | Catalytic reduction of nitrogen gas to ammonia in the presence of molybdenum complexes. **a**, Previous and current reaction systems for catalytic ammonia formation. **b**, Catalytic reduction of nitrogen gas (1 atm) in the presence of **1a** using SmI_2 and ethylene glycol in THF at room temperature. **c**, Time profile of the catalytic formation of ammonia and dihydrogen using **1a**. Data are mean of multiple individual experiments (at least 2), with error bars representing the s.d. **d**, Results of the catalytic reaction using larger amounts of SmI_2 and ethylene glycol or water in the presence of catalyst **9**. [a]Yield based on SmI_2. $SmI_2(THF)_2$ was used as the source of SmI_2.

This combination was then applied to reactions using other molybdenum complexes[7] as catalysts. Tribromide and trichloride complexes of molybdenum that bear a pyridine-based PNP-type pincer ligand $[MoX_3(PNP)]$ (**1b**, X = Br; **1c**, X = Cl) were found to be more effective catalysts than **1a** (Extended Data Table 1, entries 1 and 2). Conversely, a dinitrogen-bridged dimolybdenum complex bearing pyridine-based PNP-pincer ligands $[Mo(N_2)_2(PNP)]_2(\mu\text{-}N_2)$ (**2**) and a molybdenum trichloride complex bearing a triphosphine (PPP) ligand $[MoCl_3(PPP)]$ (**3**; PPP = bis(di-*tert*-butylphosphinoethyl)phenylphosphine) were less effective than **1a** (Extended Data Table 1, entries 3 and 4).

To obtain more information on the reaction pathway, we carried out various stoichiometric and catalytic reactions. The reaction of **1a** with 5 equiv. of SmI_2 in THF at room temperature for 5 min under 1 atm of N_2 gave the corresponding molybdenum nitride complex $[MoI(\equiv N)(PNP)]$ (**4**) in 76% yield (based on nuclear magnetic resonance (NMR) spectroscopy) (Fig. 2a). Complex **4** was previously isolated and characterized using reaction system A[7]. Notably, reactions of **1b** and **1c** gave the same complex, **4**, in yields of 74% and 85% respectively (based on NMR). This shows that molybdenum halide complexes readily underwent ligand exchange with the iodide derived from SmI_2. When **4** was allowed to react with 3 equiv. of SmI_2 and 3 equiv. of ethylene glycol in THF at room temperature for 1 h under 1 atm of argon, ammonia was produced quantitatively (Fig. 2b). Separately, we confirmed that **4** has a similar catalytic activity to **1** in the formation of ammonia (Table 1,

Table 1 | Catalytic nitrogen fixation using typical alcohols as proton sources in the presence of molybdenum complexes as catalysts

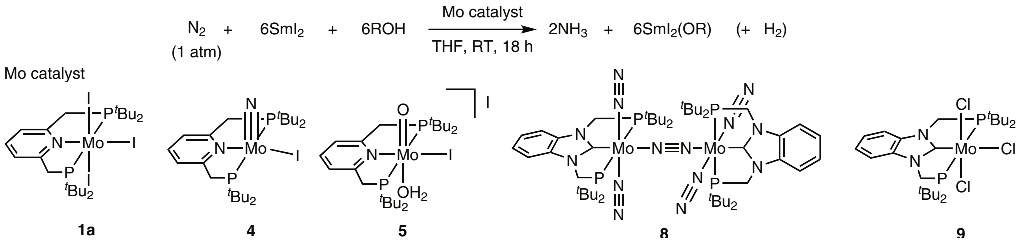

Entry	Mo catalyst	Alcohol	NH_3 production (equiv. based on Mo)	NH_3 yield (%)[a]	H_2 production (equiv. based on Mo)	H_2 yield (%)[a]
1	**1a**	$HOCH_2CH_2OH$	42.8 ± 1.5[b]	70 ± 2[b]	22.2 ± 4.5[b]	24 ± 4[b]
2	**1a**	MeOH[c]	17.2 ± 1.1[b]	28 ± 1[b]	40.7 ± 1.9[b]	44 ± 12[b]
3	**1a**	EtOH[c]	14.5	24	41.6	45
4	**1a**	^{i}PrOH[c]	11.8	19	52.2	57
5	**1a**	^{t}BuOH[c]	7.7	13	41.2	45
6	**1a**	CF_3CH_2OH[c]	13.8	22	55.4	60
7	**1a**	PhOH[c]	16.5	27	46.1	50
8	**1a**	[ColH][OTf][c]	14.4	23	63.0	68
9[d]	**1a**	$HOCH_2CH_2OH$	0	0	0	0
10	**4**	$HOCH_2CH_2OH$	50.0 ± 0.1[b]	85 ± 1[b]	7.7 ± 1.0[b]	9 ± 1[b]
11	**5**	$HOCH_2CH_2OH$	44.1	76	17.9	20
12	**8**	$HOCH_2CH_2OH$	53.3 ± 2.1[b]	88 ± 4[b]	9.1 ± 0.7[b]	10 ± 1[b]
13	**9**	$HOCH_2CH_2OH$	55.0 ± 0.9[b]	92 ± 2[b]	4.0 ± 0.8[b]	5 ± 1[b]

$SmI_2(THF)_2$ was used as the source of SmI_2.

[a] Yield based on SmI_2.

[b] Data are mean of multiple individual experiments (at least 2) with error bars representing the s.d.

[c] A proton source (0.72 mmol; 360 equiv. based on the molybdenum atom of **1a**) was used.

[d] $CoCp^*_2$ was used as the reducing reagent instead of SmI_2.

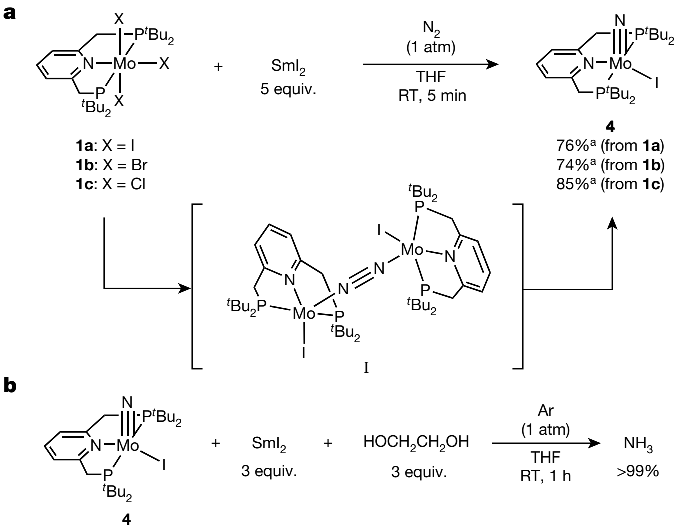

Fig. 2 | Stoichiometric reactions of ammonia formation in reaction system B. a, Stoichiometric reduction of molybdenum trihalide complexes (**1a**–**c**) to a molybdenum nitride complex (**4**) under 1 atm of N_2. **b**, Stoichiometric formation of ammonia from **4**. ^{a}Yield based on NMR. $SmI_2(THF)_2$ was used as the source of SmI_2.

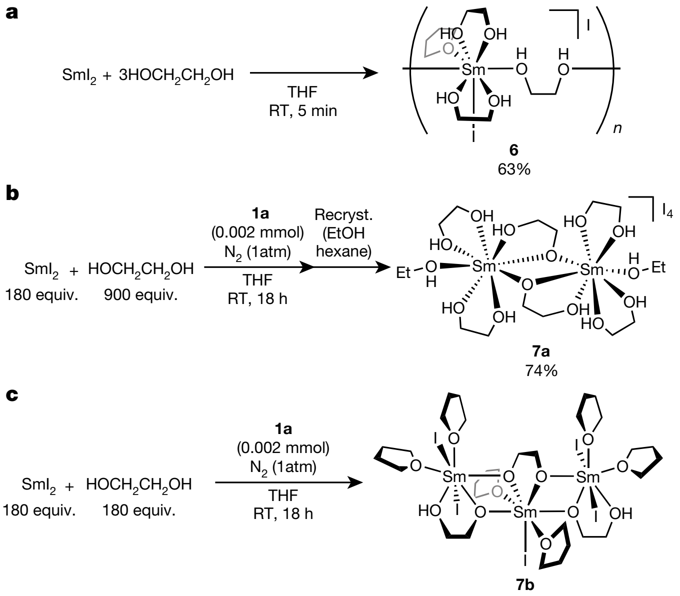

Fig. 3 | Samarium species in the catalytic reaction. a, Ethylene glycol-bridged polysamarium(II) complex (**6**) obtained from the reaction mixture using SmI_2 and 3 equiv. of ethylene glycol. **b**, Oxygen-bridged disamarium(III) complex (**7a**) obtained from the reaction mixture of the catalytic reaction using 180 equiv. (to **1a**) of SmI_2 and 900 equiv. (to **1a**) of ethylene glycol (after recrystallization from ethanol/hexane). **c**, Oxygen-bridged trisamarium (III) complex (**7b**) obtained from the reaction mixture of the catalytic reaction using 180 equiv. (to **1a**) of SmI_2 and 180 equiv. (to **1a**) of ethylene glycol. $SmI_2(THF)_2$ was used as the source of SmI_2.

entry 10), which indicates that **4** is involved as one of the key reactive intermediates in this catalytic reaction. We also confirmed that **4** was recovered unreacted from reactions using either SmI_2 or ethylene glycol.

We have observed the same result in both stoichiometric and catalytic reactions using **1** and **4** in the reaction system A[7]. On the basis of the experimental results and density functional theory calculations, we have previously proposed a reaction pathway via direct cleavage of the nitrogen–nitrogen triple bond of the bridging dinitrogen ligand in [MoI(PNP)–N≡N–MoI(PNP)] (**I**)[7] (Extended Data Fig. 1a). The results presented in this paper may suggest that ammonia formation using reaction system B proceeds via a similar pathway as reaction system A.

Next, the reactivity of a molybdenum–oxo complex was investigated in detail. The reaction of a cationic molybdenum oxo complex bearing an aqua ligand [MoI(=O)(OH_2)(PNP)]I (**5**) (Extended Data Fig. 1b) with 5 equiv. of SmI_2 in THF at room temperature for 1 h under 1 atm of N_2 gave the molybdenum nitride complex **4** in 36% yield (based on NMR). This suggests that, in the presence of SmI_2, an oxygen atom can be abstracted from **5** to give **4** via direct cleavage of the nitrogen–nitrogen triple bond of the bridging dinitrogen ligand in complex **I**. Separately, we confirmed that **5** has a similar catalytic activity to **1** and **4** under the same reaction conditions (Table 1, entry 11). This shows that the formation of molybdenum oxo complexes—including **5**—does not interfere with the formation of ammonia, even if the complexes are formed during the catalytic reaction in reaction system B.

Next, we turned our attention to the samarium species in this catalytic reaction. We did not isolate any samarium(II) complexes from the reaction of SmI_2 with the same number of equivalents of ethylene glycol in THF at room temperature. However, from the reaction of SmI_2 with 3 equiv. (to SmI_2) of ethylene glycol, we isolated (in 63% yield) an ethylene glycol-bridged polysamarium(II) complex bearing two ethylene glycol molecules and one THF molecule (**6**) (Fig. 3a). The molecular structure of **6** was confirmed by X-ray analysis. Some samarium(II) complexes with alcohols as ligands have already been prepared via the reaction of SmI_2 with various alcohols[15].

Conversely, an oxygen-bridged disamarium(III) complex (**7a**) was obtained in 74% isolated yield (after recrystallization in ethanol/hexane) from the reaction mixture of the catalytic reaction using 180 equiv. (to **1a**) of SmI_2 and 900 equiv. (to **1a**) of ethylene glycol (Fig. 3b). Additionally, an oxygen-bridged trisamarium(III) complex (**7b**) was obtained after reaction with 180 equiv. (to **1a**) of SmI_2 and 180 equiv. (to **1a**) of ethylene glycol, although we isolated only a small amount of this complex in a pure form (Fig. 3c). Detailed molecular structures of **7a** and **7b** were confirmed by X-ray analysis. In both complexes, the samarium centre had been oxidized from Sm(II) to Sm(III) together with the loss of 1 equiv. of protons (based on the samarium atom), showing that SmI_2 and ethylene glycol may formally act as a one-electron reducing reagent and also as a proton source in the process of protonation and reduction in this reaction system.

To obtain more information on the reaction pathway, we estimated the kinetic isotope effect of the catalytic reaction using deuterated ethylene glycol ($DOCH_2CH_2OD$) as a proton source. The ratio of the rate constants of the reactions involving hydrogen and deuterium (k_H/k_D) is 2.0, which is consistent with that of proton-coupled electron transfer reactions with SmI_2[18–21]. On the basis of the kinetic isotope effect and the unique reactivity of the combination of SmI_2 and ethylene glycol, we consider that ammonia formation in reaction system B proceeds via a proton-coupled electron transfer pathway[18–21] from samarium ethylene glycol complexes to nitrogenous ligands on the molybdenum atom of nitride, imide and amide complexes[3,22,23]. At present, we consider that SmI_2 and ethylene glycol are not separate electron and proton sources, but rather they work together[24–26]. Thus, we propose that ethylene glycol first coordinates to SmI_2, resulting in the weakening of the O–H bond; this enables the delivery of the hydrogen atoms to nitrogenous ligands on the molybdenum catalyst. It is known that the O–H bonds in the SmI_2–ethylene glycol complex are sufficiently reactive to enable N–H bond formation in reduced molybdenum ammine and -amide complexes[3,22,23]. For example, when water complexes with SmI_2, the effective O–H bond strength in $[Sm(H_2O)_n]^{2+}$ is 26 kcal mol^{-1} (ref. [21]), compared that of free water at 111 kcal mol^{-1} (see below).

Next we investigated catalytic reactions using other molybdenum complexes as catalysts. We recently found that a molybdenum complex bearing *N*-heterocyclic carbene- and phosphine-based PCP-pincer ligands $[Mo(N_2)_2(PCP)]_2(\mu\text{-}N_2)$ (**8**; PCP = 1,3-bis((di-*tert*-butylphosphino)methyl)benzimidazol-2-ylidene) was a more effective catalyst than molybdenum complexes bearing pyridine-based PNP-pincer ligands[27]. Accordingly, complex **8** and a molybdenum trichloride

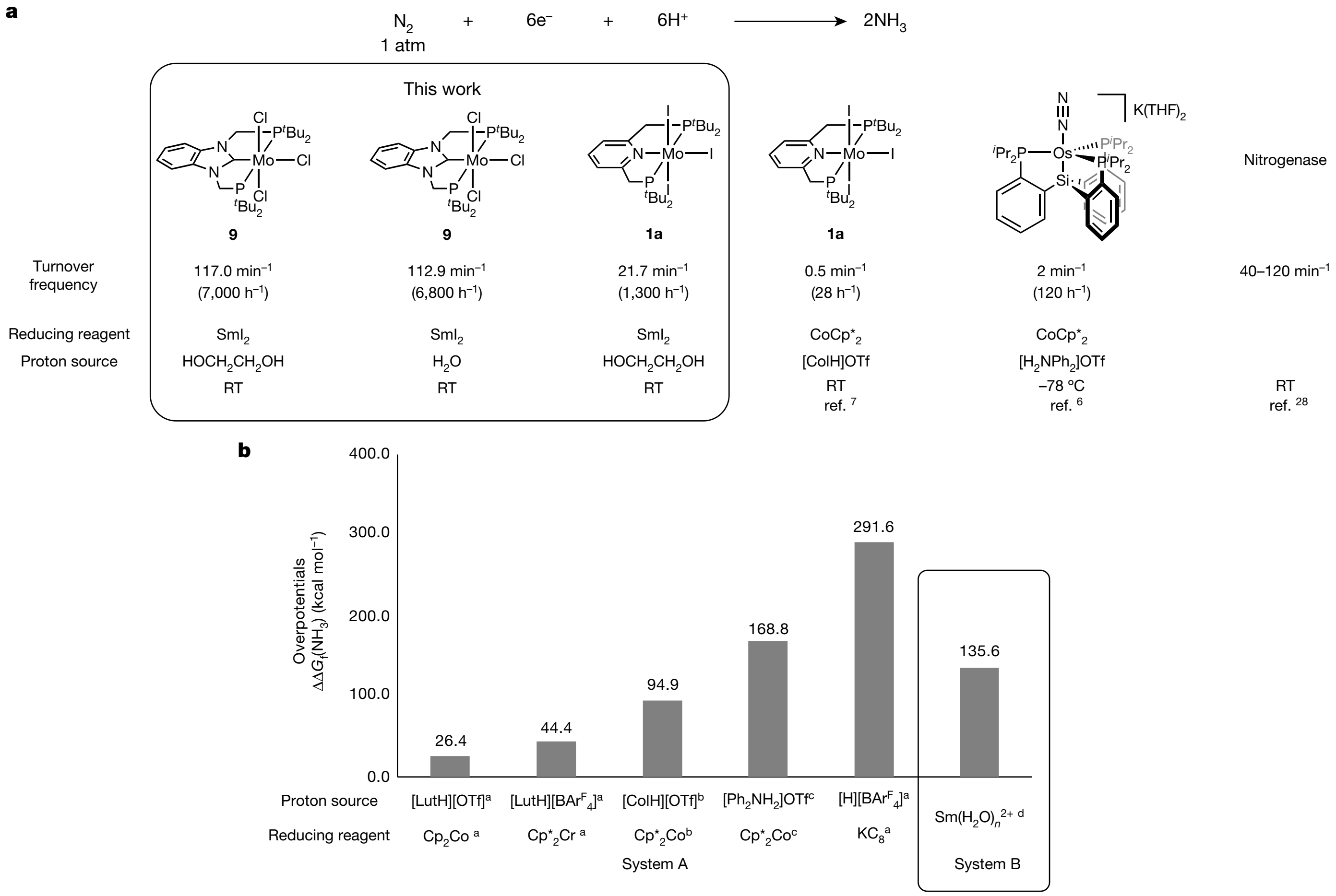

Fig. 4 | Typical turnover frequencies and chemical overpotentials. **a**, Comparison of typical TOFs obtained in the current reaction and known catalytic reactions. **b**, Chemical overpotential is calculated as 6(48.6 − BDFE), where effective bond dissociation free energy (BDFE) is calculated as 1.37(pK_a) + 23.06(E_{red}) + C (where C is the $H^+/H^\bullet$ standard reduction potential). C(MeCN) = 54.9 kcal mol^{-1} (ref. 30). Reduction potentials are corrected from the reported value according to a literature method[31]. [a]The value reported in ref. 29. [b]The system was reported by our group[7]. pK_a(MeCN) = 15.0 (ref. 32), E_{red} = −1.85 V versus Fc/Fc$^+$ (ref. 16), [c]The system was reported in ref. 6. pK_a(MeCN) = 6.0 (ref. 32), E_{red} = −1.85 V versus Fc/Fc$^+$ (ref. 16). [d]The BDFE value reported in ref. 21 (26 kcal mol^{-1}) was used.

complex bearing a PCP-type pincer ligand [$MoCl_3$(PCP)] (**9**) were found to have a similar reactivity to **1a** (Table 1, entries 12 and 13). This prompted us to carry out the catalytic reaction using larger amounts of SmI_2 and ethylene glycol in the presence of **9** as a catalyst, because the formation of only a small amount of hydrogen gas was observed when **9** was used as a catalyst. The reaction of nitrogen gas at 1 atm with 14,400 equiv. (to **9**) of SmI_2 and 14,400 equiv. (to **9**) of ethylene glycol in the presence of **9** in THF at room temperature for 4 h gave 3,650 equiv. of ammonia (based on the molybdenum atom; 76% yield based on SmI_2) (Fig. 1d). The amount of ammonia produced was ten times larger than that previously obtained[7] in reaction system A. The high performance of **9** as a catalyst prompted us to measure the TOF of **9** in reaction system B. We observed the formation of 117.0 equiv. of ammonia (based on the molybdenum atom) in 1 min, giving a TOF of 117.0 min^{-1} (7,000 h^{-1}) (Extended Data Table 5, entry 2). The result indicates that **9** has a higher catalytic performance than **1c**, in terms of both the amount of ammonia produced and its formation rate in reaction system B (see above).

Notably, the reaction of nitrogen gas at 1 atm with 14,400 equiv. (to **9**) of SmI_2 and 14,400 equiv. (to **9**) of water in the presence of **9** in THF at room temperature for 4 h gave 4,350 equiv. of ammonia (based on the molybdenum atom; 91% yield based on SmI_2) together with 150 equiv. of hydrogen gas (based on the molybdenum atom; 2% yield based on SmI_2). This indicates that water acts as a more effective proton source than alcohols in this reaction system. To our knowledge, this is the first successful example of the direct use of water as a proton source for the catalytic reduction of nitrogen gas to ammonia under ambient reaction conditions. We also observed the formation of 112.9 equiv. of ammonia (based on the molybdenum atom) in 1 min, where the TOF is 112.9 min^{-1} (6,800 h^{-1}) (Extended Data Table 5, entry 4). It is notable that the TOF observed in water (112.9 min^{-1}) is almost the same as that in ethylene glycol (117.0 min^{-1}), although the amount of ammonia produced in water (4,350 equiv.) is substantially higher than that produced in ethylene glycol (3,650 equiv).

For comparison, typical results for this reaction together with those from previous reactions[6,7] and values for nitrogenase enzymes[28] are summarized in Fig. 4a. The highest TOF (117.0 min^{-1}) was achieved using **9** as a catalyst in reaction system B, which is substantially higher than that (0.5 min^{-1}) using **1a** as a catalyst in reaction system A. A previous study has also reported the osmium-catalysed formation of ammonia under mild reaction conditions, in which the TOF is 2 min^{-1} (ref. 6). It is noteworthy that the TOF of the current reaction system (117.0 min^{-1}) is close to that observed in nitrogenase enzymes (TOF 40–120 min^{-1})[28].

Recently the energetic efficiency of ammonia formation was reported, in which the chemical overpotentials were calculated on the basis of effective bond dissociation free energy[29]. The chemical overpotential refers to excess thermodynamic driving force using the combination of a reducing reagent and a proton source in comparison to ammonia formation from hydrogen gas. Typical chemical overpotential values for ammonia formation are shown in Fig. 4b. In the reaction systems reported in refs [2,4,5], the respective values of 44.4 kcal mol^{-1}, 26.4 kcal mol^{-1} and 291.6 kcal mol^{-1} were calculated on the basis of the nature of the reducing reagents and proton sources[29]. We have also calculated the chemical overpotentials for the current reaction system B. The pK_a of water reduces upon coordination and, in combination with a reducing Sm(II)/Sm(III) couple, results in an effective O–H bond strength of 26 kcal mol^{-1} (ref. [21]) in $[Sm(H_2O)_n]^{2+}$, compared to an O–H bond dissociation free energy of 111 kcal mol^{-1} in free water. When the effective value for $[Sm(H_2O)_n]^{2+}$ is used, the calculated chemical overpotential value is 135.6 kcal mol^{-1}. Although this value is very far from the ideal reaction, this presents an opportunity for further research in the field of catalytic nitrogen fixation.

Online content

Any methods, additional references, Nature Research reporting summaries, source data, statements of data availability and associated accession codes are available at https://doi.org/10.1038/s41586-019-1134-2.

Received: 14 August 2018; Accepted: 28 February 2019;
Published online 24 April 2019.

1. Liu, H. *Ammonia Synthesis Catalysts: Innovation and Practice* (World Scientific, Beijing, 2013).
2. Yandulov, D. V. & Schrock, R. R. Catalytic reduction of dinitrogen to ammonia at a single molybdenum center. *Science* **301**, 76–78 (2003).
3. Nishibayashi, Y. (ed.) *Nitrogen Fixation (Topics in Organometallic Chemistry)* 1st edn, Vol. 60 (Springer, Heidelberg, 2017).
4. Arashiba, K., Miyake, Y. & Nishibayashi, Y. A molybdenum complex bearing PNP-type pincer ligands leads to the catalytic reduction of dinitrogen into ammonia. *Nat. Chem*. **3**, 120–125 (2011).
5. Anderson, J. S., Rittle, J. & Peters, J. C. Catalytic conversion of nitrogen to ammonia by an iron model complex. *Nature* **501**, 84–87 (2013).
6. Fajardo, J. Jr & Peters, J. C. Catalytic nitrogen-to-ammonia conversion by osmium and ruthenium complexes. *J. Am. Chem. Soc*. **139**, 16105–16108 (2017).
7. Arashiba, K. et al. Catalytic nitrogen fixation via direct cleavage of nitrogen–nitrogen triple bond of molecular dinitrogen under ambient reaction conditions. *Bull. Chem. Soc. Jpn* **90**, 1111–1118 (2017).
8. Karunadasa, H. I., Chang, C. J. & Long, J. R. A molecular molybdenum-oxo catalyst for generating hydrogen from water. *Nature* **464**, 1329–1333 (2010).
9. Chatt, J., Pearman, A. J. & Richards, R. L. The reduction of mono-coordinated molecular nitrogen to ammonia in a protic environment. *Nature* **253**, 39–40 (1975).
10. Ohki, Y., Aoyagi, K. & Seino, H. Synthesis and protonation of N-heterocyclic-carbene-supported dinitrogen complexes of molybdenum(0). *Organometallics* **34**, 3414–3420 (2015).
11. Li, H., Shang, J., Ai, Z. & Zhang, L. Efficient visible light nitrogen fixation with BiOBr nanosheets of oxygen vacancies on the exposed {001} facets. *J. Am. Chem. Soc*. **137**, 6393–6399 (2015).
12. Hirakawa, H., Hashimoto, M., Shiraishi, Y. & Hirai, T. Photocatalytic conversion of nitrogen to ammonia with water on surface oxygen vacancies of titanium dioxide. *J. Am. Chem. Soc*. **139**, 10929–10936 (2017).
13. Szostak, M., Fazakerley, N. J., Parmar, D. & Procter, D. J. Cross-coupling reactions using samarium(II) iodide. *Chem. Rev*. **114**, 5959–6039 (2014).
14. Choquette, K. A. & Flowers, R. A. in *Comprehensive Organic Synthesis II* Vol. 1 (eds Knochel, P. & Molander, G. A.) Ch. 9, 278–343 (Elsevier, Amsterdam, 2014).
15. Teprovich, J. A. Jr, Balili, M. N., Pintauer, T. & Flowers, R. A. II. Mechanistic studies of proton-donor coordination to samarium diiodide. *Angew. Chem. Int. Ed*. **46**, 8160–8163 (2007).
16. Robbins, J. L., Edelstein, N., Spencer, B. & Smart, J. C. Syntheses and electronic structures of decamethylmetallocenes. *J. Am. Chem. Soc*. **104**, 1882–1893 (1982).
17. Kuhlman, M. L. & Flowers R. A. II. Aggregation state and reducing power of the samarium diiodide–DMPU complex in acetonitrile. *Tetrahedron Lett*. **41**, 8049–8052 (2000).
18. Chciuk, T. V., Anderson, W. R. Jr & Flowers, R. A. II. High-affinity proton donors promote proton-coupled electron transfer by samarium diiodide. *Angew. Chem. Int. Ed*. **55**, 6033–6036 (2016).
19. Chciuk, T. V., Anderson, W. R. Jr & Flowers, R. A. II. Proton-coupled electron transfer in the reduction of carbonyls by samarium diiodide–water complexes. *J. Am. Chem. Soc*. **138**, 8738–8741 (2016).
20. Chciuk, T. V., Anderson, W. R. Jr & Flowers, R. A. II. Interplay between substrate and proton donor coordination in reductions of carbonyls by SmI_2–water through proton-coupled electron-transfer. *J. Am. Chem. Soc*. **140**, 15342–15352 (2018).
21. Kolmar, S. S. & Mayer, J. M. $SmI_2(H_2O)_n$ reduction of electron rich enamines by proton-coupled electron transfer. *J. Am. Chem. Soc*. **139**, 10687–10692 (2017).
22. Bezdek, M. J., Guo, S. & Chirik, P. J. Coordination-induced weakening of ammonia, water, and hydrazine X–H bonds in a molybdenum complex. *Science* **354**, 730–733 (2016).
23. Bezdek, M. J. & Chirik, P. J. Interconversion of molybdenum imido and amido complexes by proton-coupled electron transfer. *Angew. Chem. Int. Ed*. **57**, 2224–2228 (2018).
24. Jonas, R. T. & Stack, T. D. P. C–H bond activation by a ferric methoxide complex: a model for the rate-determining step in the mechanism of lipoxygenase. *J. Am. Chem. Soc*. **119**, 8566–8567 (1997).
25. Spiegel, D. A., Wiberg, K. B., Schacherer, L. N., Medeiros, M. R. & Wood, J. L. Deoxygenation of alcohols employing water as the hydrogen atom source. *J. Am. Chem. Soc*. **127**, 12513–12515 (2005).
26. Pozzi, D., Scanlan, E. M. & Renaud, P. A mild radical procedure for the reduction of *B*-alkylcatecholboranes to alkanes. *J. Am. Chem. Soc*. **127**, 14204–14205 (2005).
27. Eizawa, A. et al. Remarkable catalytic activity of dinitrogen-bridged dimolybdenum complexes bearing NHC-based PCP-pincer ligands toward nitrogen fixation. *Nat. Commun*. **8**, 14874 (2017).
28. Brown, K. A. et al. Light-driven dinitrogen reduction catalyzed by a CdS:nitrogenase MoFe protein biohybrid. *Science* **352**, 448–450 (2016).
29. Pappas, I. & Chirik, P. J. Catalytic proton coupled electron transfer from metal hydrides to titanocene amides, hydrazides and imides: determination of thermodynamic parameters relevant to nitrogen fixation. *J. Am. Chem. Soc*. **138**, 13379–13389 (2016).
30. Warren, J. J., Tronic, T. A. & Mayer, J. M. Thermochemistry of proton-coupled electron transfer reagents and its implications. *Chem. Rev*. **110**, 6961–7001 (2010).
31. Pavlishchuk, V. V. & Addison, A. W. Conversion constants for redox potentials measured versus different reference electrodes in acetonitrile solutions at 25 °C. *Inorg. Chim. Acta* **298**, 97–102 (2000).
32. Kaljurand, I. et al. Extension of the self-consistent spectrophotometric basicity scale in acetonitrile to a full span of 28 pK_a units: unification of different basicity scales. *J. Org. Chem*. **70**, 1019–1028 (2005).

Acknowledgements This project is supported by CREST, JST (JPMJCR1541). We thank Grants-in-Aid for Scientific Research (numbers JP17H01201, JP15H05798 and JP18K19093) from JSPS and MEXT. Y.A. is a recipient of the JSPS Predoctoral Fellowships for Young Scientists. We also thank J. C. Peters and S. Schneider for helpful discussions.

Reviewer information *Nature* thanks Robert Flowers and the other anonymous reviewer(s) for their contribution to the peer review of this work.

Author contributions Y.N. directed and conceived this project. Y.A., K.A. and K.N. conducted the experimental work including X-ray analysis. All authors discussed the results and wrote the manuscript.

Competing interests Y.A., K.N. and Y.N. have filed a patent based on the work described here (Japanese patent application number 2018-036967).

Additional information
Extended data is available for this paper at https://doi.org/10.1038/s41586-019-1134-2.
Reprints and permissions information is available at http://www.nature.com/reprints.
Correspondence and requests for materials should be addressed to Y.N.
Publisher's note: Springer Nature remains neutral with regard to jurisdictional claims in published maps and institutional affiliations.

METHODS

General methods. All manipulations were carried out under an atmosphere of nitrogen or argon by using standard Schlenk techniques or glove-box techniques unless otherwise stated. All solvents were dried by general methods and degassed before use. $[MoI_3(PNP)]$ (**1a**)[7], $[MoBr_3(PNP)]$ (**1b**)[7], $[MoCl_3(PNP)]$ (**1c**)[4], $[Mo(N_2)_2(PNP)]_2(\mu\text{-}N_2)$ (**2**)[4], $[MoCl_3(PPP)]$ (**3**)[33], $[MoI(\equiv N)(PNP)]$ (**4**)[7], $[Mo(N_2)_2(PCP)]_2(\mu\text{-}N_2)$ (**8**)[27], $[MoCl_3(PCP)]$ (**9**)[27], $[SmI_2(THF)_2]$[34], [ColH]OTf (ref. [33]) and $CoCp^*_2$ (ref. [35]) were prepared according to the literature methods. Other reagents were purchased commercially and used as received.

^1H NMR (400 MHz), $^{31}P\{^1H\}$ NMR (162 MHz), and $^{15}N\{^1H\}$ NMR (41 MHz) spectra were recorded on a JEOL ECS400 spectrometer in suitable solvents, and spectra were referenced to residual solvent (^1H) or external standard ($^{31}P\{^1H\}$: 85% H_3PO_4, $^{15}N\{^1H\}$: CH_3NO_2). Ultraviolet–visible (UV–vis) absorption spectra were recorded on a Shimadzu MultiSpec-1500 and a Shimadzu UV-1850. Mass spectra were recorded on a JEOL Accu TOF JMS-T100LP. Evolved dihydrogen was quantified by gas chromatography (GC) using a Shimadzu GC-8A equipped with a thermal conductivity detector and a ShinCarbon ST column (6 m × 3 mm). Elemental analyses were performed at Microanalytical Center of The University of Tokyo.

Catalytic reduction of dinitrogen to ammonia with alcohols. A typical experimental procedure for the catalytic reactions is described below. In a nitrogen-filled glove box, to a mixture of **1a** (1.7 mg, 0.0020 mmol) and $SmI_2(THF)_2$ (198 mg, 0.361 mmol) placed in a 50 ml Schlenk flask was added THF (6 ml). Next, ethylene glycol (20 μl, 0.36 mmol) was added in one portion, and the mixture was stirred at room temperature for 30 min. After the reaction, the amount of generated dihydrogen (0.0291 mmol, 14.9 equiv. based on the molybdenum atom, 16% yield based on $SmI_2(THF)_2$) was quantified by GC. Aqueous potassium hydroxide solution (30 wt%, 5 ml) was added to the reaction mixture. The mixture was evaporated under reduced pressure, and the distillate was trapped in a dilute H_2SO_4 solution (0.5 M, 10 ml). The amount of ammonia (0.0839 mmol, 43.1 equiv. based on the molybdenum atom, 70% yield based on $SmI_2(THF)_2$) present in the H_2SO_4 solution was determined by the indophenol method[36]. No hydrazine was detected by the *p*-(dimethylamino)benzaldehyde method[37]. The consumption of SmI_2 was confirmed by the colour change of the reaction mixture from deep blue to yellow.

Catalytic reactions in various solvents were carried out using the typical experimental procedure (Extended Data Table 2).

After the catalytic reaction, we tried to identify the resting state of molybdenum complexes. Only the formation of molybdenum nitride complex $[Mo(\equiv N)I(PNP)]$ (**4**) was observed from the reaction mixture by electrospray ionization time-of-flight mass spectrometry (ESI-TOF-MS) ($m/z = 634$). No identified molybdenum complexes except for **4** were observed by NMR and electron paramagnetic resonance spectroscopies.

Catalytic reduction of dinitrogen to ammonia under $^{15}N_2$. In a 50 ml Schlenk flask were placed **1c** (1.2 mg, 0.0020 mmol) and $SmI_2(THF)_2$ (197 mg, 0.360 mmol). The flask was evacuated and backfilled with $^{15}N_2$. Then ethylene glycol (20 μl, 0.36 mmol) in THF (6 ml) was added to the stirred solution in the Schlenk flask in one portion, and the mixture was stirred at room temperature for 18 h. KO^tBu (4 mmol) in MeOH (5 ml) was added to the resultant yellow solution, and the mixture was stirred at room temperature for 20 min. The volatile components in the mixture were collected by trap-to-trap distillation to the Schlenk flask to which was added a solution of 2 M HCl in Et_2O (5 ml, 10 mmol). The obtained colourless solution was dried in vacuo to afford a colourless solid which contained $^{15}NH_4Cl$. The amount of $^{15}NH_4Cl$ (0.0797 mmol, 39.7 equiv. based on the molybdenum atom, 67% NMR yield based on $SmI_2(THF)_2$) was determined by ^1H NMR in DMSO-d_6 with 1,1,2,2-tetrachloroethane as an internal standard and [ColH][OTf] as an acid. The ^1H NMR spectrum of this solid is shown in Extended Data Fig. 2. ^1H NMR (DMSO-d_6): δ 7.32 (d, $J_{NH} = 71.6$ Hz, $^{15}NH_4Cl$). $^{15}N\{^1H\}$ NMR (DMSO-d_6): δ −355.7 (s, $^{15}NH_4Cl$).

Reaction of 1 **with 5 equivalents of $SmI_2(THF)_2$ under N_2.** A mixture of **1a** (8.7 mg, 0.010 mmol) and $SmI_2(THF)_2$ (27.6 mg, 0.050 mmol) in THF (2 ml) placed in a 20 ml Schlenk flask was stirred at room temperature for 5 min under N_2 (1 atm). After volatiles were removed in vacuo, formation of **4** was confirmed by ^1H NMR and ESI-TOF-MS[7]. The NMR yield of **4** (0.0076 mmol, 76%) in the residual solid was determined with hexamethylbenzene as an internal standard. Separately, we observed the formation of the ^{15}N-labelled molybdenum nitride complex $[MoI(\equiv{}^{15}N)(PNP)]$ (**4′**) by ESI-TOF-MS analysis from the reaction of **1a** with 5 equiv. of SmI_2 under 1 atm of $^{15}N_2$ gas.

When **1b** was used as a starting material, the yield of **4** in the residual solid was 0.0074 mmol (74% NMR yield). When **1c** was used as a starting material, the yield of **4** in the residual solid was 0.0086 mmol (85% NMR yield).

Reaction of 4 **with 3 equivalents of $SmI_2(THF)_2$ and 3 equivalents of ethylene glycol under argon.** In an argon-filled glove box, to a mixture of **4** (25.4 mg, 0.0402 mmol) and $SmI_2(THF)_2$ (65.8 mg, 0.120 mmol) placed in a 50 ml Schlenk flask was added THF (3 ml). Then THF solution (3 ml) containing ethylene glycol (0.12 mmol) was added to the stirred solution in the Schlenk flask in one portion, and the mixture was stirred at room temperature for 2 h. After the reaction, the amount of generated dihydrogen (0.0284 mmol, 47% yield based on $SmI_2(THF)_2$) was quantified by GC. The amount of ammonia (0.0416 mmol, >99% yield based on $SmI_2(THF)_2$) was determined by the indophenol method[36].

Reaction of 4 **with 1 equivalent of $SmI_2(THF)_2$ or 1 equivalent of ethylene glycol under argon.** In an argon-filled glove box, to a mixture of **4** (1.6 mg, 0.0025 mmol) and triphenylphosphine as an internal standard in an NMR sample tube was added THF (0.5 ml). Then THF solution (0.1 ml) containing ethylene glycol (0.0025 mmol) or $SmI_2(THF)_2$ (0.0025 mmol) was added to the solution. No consumption of **4** was detected by $^{31}P\{^1H\}$ NMR in THF.

Preparation of $[Mo(O)I(PNP)(H_2O)]I$ (5). To a solution of $[MoI_3(PNP)]$ (**1a**) (174 mg, 0.199 mmol) in THF (16 ml) were added pyridine (38.0 μl, 0.473 mmol) and water (7.0 μl, 0.39 mmol) under a nitrogen atmosphere, and the mixture was stirred at 50 °C for 14 h (Extended Data Fig. 1b). The resultant yellow-green suspension was concentrated under reduced pressure, then the residue was washed with benzene (5 ml × 3). Volatiles were removed in vacuo, and THF (5 ml) was added to the residue. The THF solution was filtered through Celite, the filter cake was washed with THF (5 ml × 1), and the combined filtrate was concentrated under reduced pressure. To the residue was added CH_2Cl_2 (4 ml), then slow addition of hexane (20 ml) afforded **5** as dark yellow crystals, which were collected by filtration, washed with hexane (5 ml × 3) and Et_2O (5 ml × 3), and dried in vacuo (46.1 mg, 0.0591 mmol, 30% yield). ^1H NMR (THF-d_8): δ 7.96 (t, $J = 7.9$ Hz, Ar*H*, 1H), 7.78 (d, $J = 7.9$ Hz, Ar*H*, 2H), 6.10 (br, OH_2, 2H), 4.81–4.72 (m, CH_2P, 2H), 3.94–3.88 (m, CH_2P, 2H), 1.47 (pseudo t, $J = 6.6$ Hz, P^tBu_2, 18H), 1.40 (pseudo t, $J = 6.6$ Hz, P^tBu_2, 18H). $^{31}P\{^1H\}$ NMR (THF-d_8): δ 56.9 (s). ESI-TOF-MS (THF): 636 (m/z). Anal calcd for $C_{23}H_{45}I_2MoNO_2P_2$: C, 35.45; H, 5.82; N, 1.80. Found: C, 35.24; H, 5.56; N, 1.84. Pyridine acted as a base to deprotonate water to produce the corresponding molybdenum oxo-aquo complex **5**.

Reaction of 5 **with 5 equiv. of $SmI_2(THF)_2$ under N_2.** A mixture of **5** (3.9 mg, 0.0050 mmol) and $SmI_2(THF)_2$ (13.7 mg, 0.0250 mmol) in THF (1 ml) placed in a 20 ml Schlenk flask was stirred at room temperature for 1 h under N_2 (1 atm) (Extended Data Fig. 1b). After volatiles were removed in vacuo, the yield of $[Mo(\equiv N)I(PNP)]$ (**4**)[7] (0.0018 mmol, 36%) in the residual solid was determined by ^1H NMR in THF-d_8 with hexamethylbenzene as an internal standard. Separately, we observed the formation of ^{15}N-labelled molybdenum nitride complex $[MoI(\equiv{}^{15}N)(PNP)]$ (**4′**) by ESI-TOF-MS analysis from the reaction of $[MoI(=O)(OH_2)(PNP)]I$ (**5**) with 10 equiv. of SmI_2 under 1 atm of $^{15}N_2$ gas.

Preparation of ethylene glycol-bridged polysamarium(II) complex (6). In an argon-filled glove box, to a solution of $SmI_2(THF)_2$ (197 mg, 0.360 mmol) in THF (3.5 ml) placed in a 20 ml Schlenk flask was added ethylene glycol (60.0 μl, 1.08 mmol) in one portion. The mixture was stirred at room temperature for 5 min. After the solution was cooled and kept at −30 °C for 4 days, green crystals were formed. The crystals were washed with Et_2O (2 ml × 3) and dried under vacuum to afford **6**·C_4H_8O (165 mg, 0.225 mmol, 63% yield). Anal calcd for $C_{10}H_{26}I_2O_7Sm\cdot C_4H_8O$: C, 22.89; H, 4.67. Found: C, 23.24; H, 4.47. A single crystal suitable for X-ray analysis was obtained by heat recrystallization from a THF solution of a reaction mixture of $SmI_2(THF)_2$ and ethylene glycol at −30 °C for 4 days.

Preparation of oxygen-bridged disamarium(III) complex (7a). In a nitrogen-filled glove box, to a mixture of **1a** (1.7 mg, 0.0020 mmol) and $SmI_2(THF)_2$ (197 mg, 0.360 mmol) placed in a 50 ml Schlenk flask was added THF (6 ml). Then ethylene glycol (100 μl, 1.80 mmol) was added to the stirred solution in the Schlenk flask in one portion, and the mixture was stirred at room temperature for 18 h. After volatiles were removed in vacuo, the solid was extracted with EtOH (5 ml). Slow addition of hexane (30 ml) to the EtOH solution afforded **7a** as colourless crystals, which were collected by filtration, washed with hexane (5 ml × 3) and dried in vacuo (169 mg, 0.133 mmol, 74% yield). Anal calcd for $C_{16}H_{46}I_4O_{14}Sm_2$: C, 15.12; H, 3.65. Found: C, 14.84; H, 3.72. A single crystal suitable for X-ray analysis was obtained by two-layer recrystallization by the slow addition of hexane (30 ml) to a EtOH (5 ml) solution of **7a**.

Preparation of oxygen-bridged trisamarium(III) complex (7b). In a nitrogen-filled glove box, to a mixture of **1a** (1.7 mg, 0.0020 mmol) and $SmI_2(THF)_2$ (197 mg, 0.360 mmol) placed in a 50 ml Schlenk flask was added THF (6 ml). Then ethylene glycol (20 μl, 0.36 mmol) was added to the stirred solution in the Schlenk flask in one portion, and the mixture was stirred at room temperature for 18 h. After the reaction, slow addition of hexane (40 ml) to the reaction mixture afforded **7a** as colourless crystals for X-ray analysis. These crystals contain a small amount of **7b**·$2C_4H_8O$.

Kinetic study of catalytic reactions and stoichiometric. Kinetic study of the catalytic reaction was carried out by tracing the consumption of SmI_2 by UV–vis absorption spectroscopy at room temperature. A typical procedure is described below. A THF solution containing SmI_2 (6.0 μmol) and ethylene glycol (6.0 μmol) was added into a quartz glass cell (1 cm × 1 cm × 4 cm) with a septum in a nitrogen-filled glove box. The THF solution of **1a** (0.3 μmol) was added to the quartz glass cell using a syringe with stirring. The total amount of solution was adjusted to be 3.0 ml. The absorbance of SmI_2 at 560 nm was measured for 5 min. The k_H/k_D value of 2.0 was calculated from the consumption of SmI_2 during the period from 10 to 20 s after the start of the reaction by using $HOCH_2CH_2OH$ and $DOCH_2CH_2OD$ as proton sources under typical analytical conditions described above.

To obtain more information on the proposed reaction pathway, we carried out kinetic studies at different initial concentrations of **1a** for the stoichiometric reaction of **1a** with 2.5 equiv. of SmI_2 under 1 atm of N_2 gas to **4**. We observed a second-order rate dependence on **1a** in the stoichiometric reaction (Extended Data Fig. 3). This indicates that the formation of the dinitrogen-bridged dimolybdenum complex may be involved as the rate-determining step of the stoichiometric reaction.

Catalytic reduction of dinitrogen to ammonia with water. A typical experimental procedure for catalytic reduction with water is described below. To **1a** (1.7 mg, 0.0020 mmol) and $SmI_2(THF)_2$ (199 mg, 0.363 mmol) placed in a 50 ml Schlenk flask was added THF (4 ml) under N_2. Then THF solution (2 ml) containing H_2O (0.36 mmol) was slowly added to the stirred solution in the Schlenk flask with a syringe pump over a period of 0.5 h. After the addition of the water, the mixture was further stirred at room temperature for 17.5 h. After the reaction, the amount of generated dihydrogen (0.0702 mmol, 36.0 equiv. based on the molybdenum atom, 39% yield based on $SmI_2(THF)_2$) of the catalytic reaction was quantified by GC. Aqueous potassium hydroxide solution (30 wt%, 5 ml) was added to the reaction mixture. The mixture was evaporated under reduced pressure, and the distillate was trapped in a dilute H_2SO_4 solution (0.5 M, 10 ml). The amount of ammonia (0.0522 mmol, 26.8 equiv. based on the molybdenum atom, 43% yield based on $SmI_2(THF)_2$) present in the H_2SO_4 solution was determined by the indophenol method[36]. The results of the catalytic reactions using various molybdenum complexes as catalysts are described in Extended Data Table 3.

Catalytic reactions using larger amounts of reducing reagent and proton source. When ethylene glycol was used as a proton source, catalytic reactions were performed using smaller amount of catalysts for 4 h using the typical experimental procedure. When water was used as a proton source, the experimental procedure for the catalytic reactions is described below. To **9** (0.016 μg, 0.025 μmol) and $SmI_2(THF)_2$ (197 mg, 0.359 mmol) placed in a 50 ml Schlenk flask was added THF (1 ml) under N_2. Then THF solution (2 ml) containing H_2O (0.36 mmol) was slowly added to the stirred solution in the Schlenk flask with a syringe pump over a period of 1 h. After the addition of the H_2O, the mixture was further stirred at room temperature for 3 h. After the reaction, the amount of generated dihydrogen (0.0017 mmol, 69 equiv. based on the molybdenum atom, 1% yield based on $SmI_2(THF)_2$) of the catalytic reaction was quantified by GC. Aqueous potassium hydroxide solution (30 wt%, 5 ml) was added to the reaction mixture. The mixture was evaporated under reduced pressure, and the distillate was trapped in a dilute H_2SO_4 solution (0.5 M, 10 ml). The amount of ammonia (0.111 mmol, 4,440 equiv. based on the molybdenum atom, 88% yield based on $SmI_2(THF)_2$) present in the H_2SO_4 solution was determined by the indophenol method[36]. The results are shown in Extended Data Table 4.

Catalytic reactions to determine turnover frequencies. When ethylene glycol was used as a proton source, catalytic reactions were performed for 1 min using the typical experimental procedure. In the case that water was used as a proton source, the experimental procedure for the catalytic reactions is descried below. To **9** (0.6 mg, 0.0009 mmol) and $SmI_2(THF)_2$ (198 mg, 0.361 mmol) placed in a 50 ml Schlenk flask was added THF (1 ml) under N_2. Then THF solution (2 ml) containing H_2O (0.36 mmol) was added in one portion, and the mixture was stirred at room temperature for 1 min. After the reaction, aqueous potassium hydroxide solution (30 wt%, 5 ml) was added to the reaction mixture. The mixture was evaporated under reduced pressure, and the distillate was trapped in a dilute H_2SO_4 solution (0.5 M, 10 ml). The amount of ammonia (0.106 mmol, 112.9 equiv. based on the molybdenum atom, 88% yield based on $SmI_2(THF)_2$) present in the H_2SO_4 solution was determined by the indophenol method[36]. The results are shown in Extended Data Table 5.

Catalytic reduction of hydrazine to ammonia under argon. In an argon-filled glove box, to a mixture of **1a** (1.7 mg, 0.0020 mmol) and $SmI_2(THF)_2$ (197 mg, 0.360 mmol) placed in a 50 ml Schlenk flask was added THF (4 ml). Then THF solution (2 ml) containing hydrazine (0.06 mmol) and ethylene glycol (0.06 mmol) was added to the mixture, and the reaction mixture was stirred at room temperature for 18 h. After the reaction, the amount of generated dihydrogen (0.0097 mmol, 5.0 equiv. based on the molybdenum atom, 16% yield based on $SmI_2(THF)_2$) was quantified with GC. The amount of ammonia (0.0995 mmol, 50.0 equiv. based on the molybdenum atom, 83% yield based on hydrazine) was determined by the indophenol method[36]. The amount of hydrazine (0.00585 mmol, 10% recovery) was determined by the *p*-(dimethylamino)benzaldehyde method[37]. When the catalytic reaction was performed in the absence of **1a**, the amount of ammonia was 0.0434 mmol (36% yield based on hydrazine). The results are shown in Extended Data Table 6.

X-ray crystallography. Diffraction data for **5**, **6**, **7a** and **7b**·$2C_4H_8O$ were collected for the 2θ range of 4° to 55° on a Rigaku RAXIS RAPID imaging plate area detector with graphite-monochromated Mo Kα radiation ($\lambda = 0.71075$ Å), with VariMax optics. Intensity data were corrected for Lorenz-polarization effects and for empirical absorption (ABSCOR). The structure solution and refinements were carried out by using the *CrystalStructure* crystallographic software package[38]. The positions of non-hydrogen atoms were determined by direct methods (SIR 97[39] for **5**, **7a**, **7b**·$2C_4H_8O$ and SHELXS[40] for **6**) and subsequent Fourier syntheses (SHELXL version 2016/6[41]) and were refined on F_o^2 using all unique reflections by full-matrix least-squares with anisotropic thermal parameters. All the hydrogen atoms were placed at the calculated positions with fixed isotropic parameters, except for the H(1) and H(5) atoms in **5**, the H(9), H(10) and H(11) atoms in **7a** and the H(39) and H(40) atoms in **7b**·$2C_4H_8O$. The positions of the H(1) and H(5) atoms in **5**, the H(9), H(10) and H(11) atoms in **7a** and the H(39) and H(40) atoms in **7b**·$2C_4H_8O$ were determined on appropriate peaks in the difference Fourier maps and further refined isotropically. The crystal of **6** is a merohedral twin with a minor component comprising 3.15% of the crystal.

Data availability

Crystallographic data for the reported structures have been deposited at the Cambridge Crystallographic Data Centre, under deposition numbers: CCDC 185998 (**5**), 1857999 (**6**), 1858000 (**7a**) and 1858001 (**7b**·$2C_4H_8O$). All other data supporting the findings of this study are available within the paper or from the corresponding author upon reasonable request.

33. Arashiba, K. et al. Catalytic reduction of dinitrogen to ammonia by use of molybdenum–nitride complexes bearing a tridentate triphosphine as catalysts. *J. Am. Chem. Soc.* **137**, 5666–5669 (2015).
34. Watson, P. L., Tulip, T. H. & Williams, I. Defluorination of perfluoroolefins by divalent lanthanoid reagents: activating C–F bonds. *Organometallics* **9**, 1999–2009 (1990).
35. Yandulov, D. V. & Schrock, R. R. Synthesis of tungsten complexes that contain hexaisopropylterphenyl-substituted triamidoamine ligands, and reactions relevant to the reduction of dinitrogen to ammonia. *Can. J. Chem.* **83**, 341–357 (2005).
36. Weatherburn, M. W. Phenol-hypochlorite reaction for determination of ammonia. *Anal. Chem.* **39**, 971–974 (1967).
37. Watt, G. W. & Chrisp, J. D. Spectrophotometric method for determination of hydrazine. *Anal. Chem.* **24**, 2006–2008 (1952).
38. CrystalStructure v.4.3.: Single Crystal Structure Analysis Software (Rigaku Corp., Tokyo and MSC, Texas, 2018).
39. Altomare, A. et al. SIR97: a new tool for crystal structure determination and refinement. *J. Appl. Crystallogr.* **32**, 115–119 (1999).
40. Sheldrick, G. M. A short history of SHELX. *Acta Crystallogr. A* **64**, 112–122 (2008).
41. Sheldrick, G. M. Crystal structure refinement with SHELXL. *Acta Crystallogr. C* **71**, 3–8 (2015).

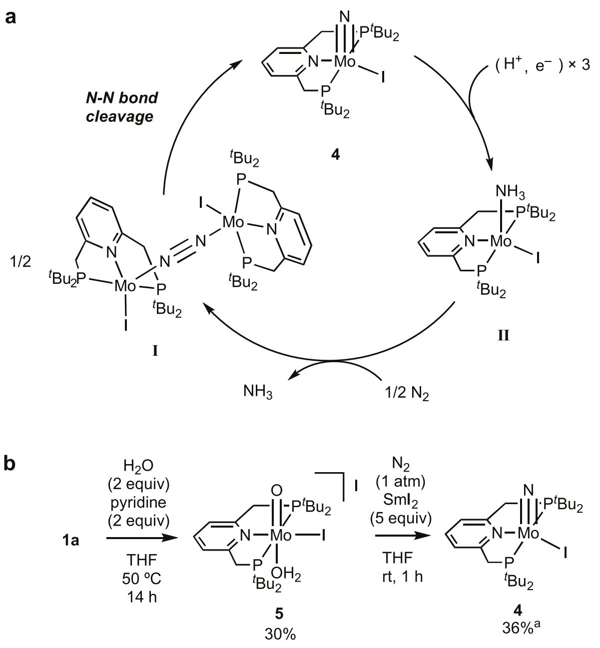

Extended Data Fig. 1 | Reactions via direct nitrogen cleavage pathway. **a**, A reaction pathway via direct cleavage of the nitrogen–nitrogen triple bond. **b**, Synthesis of the molybdenum oxo complex (**5**) from **1a** and water, and reduction of **5** to **4** via direct nitrogen cleavage of the nitrogen–nitrogen triple bond. $SmI_2(THF)_2$ was used as the source of SmI_2.[a] Yield based on NMR.

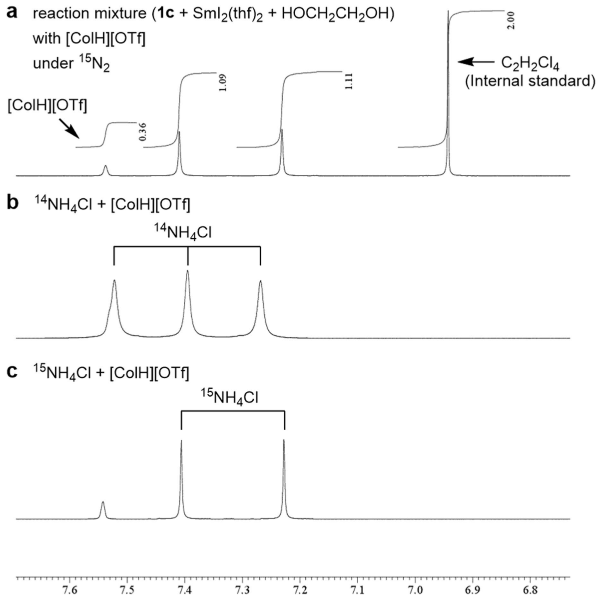

Extended Data Fig. 2 | ^{1}H NMR spectra of catalytic reduction of dinitrogen to ammonia under $^{15}N_2$. a–c, ^{1}H NMR (DMSO-d_6) spectra of product from catalytic reaction with **1c** under $^{15}N_2$ and [ColH]OTf (**a**), authentic sample of the mixture of $^{14}NH_4Cl$ and [ColH]OTf (**b**) and authentic sample of the mixture of $^{15}NH_4Cl$ and [ColH]OTf (**c**).

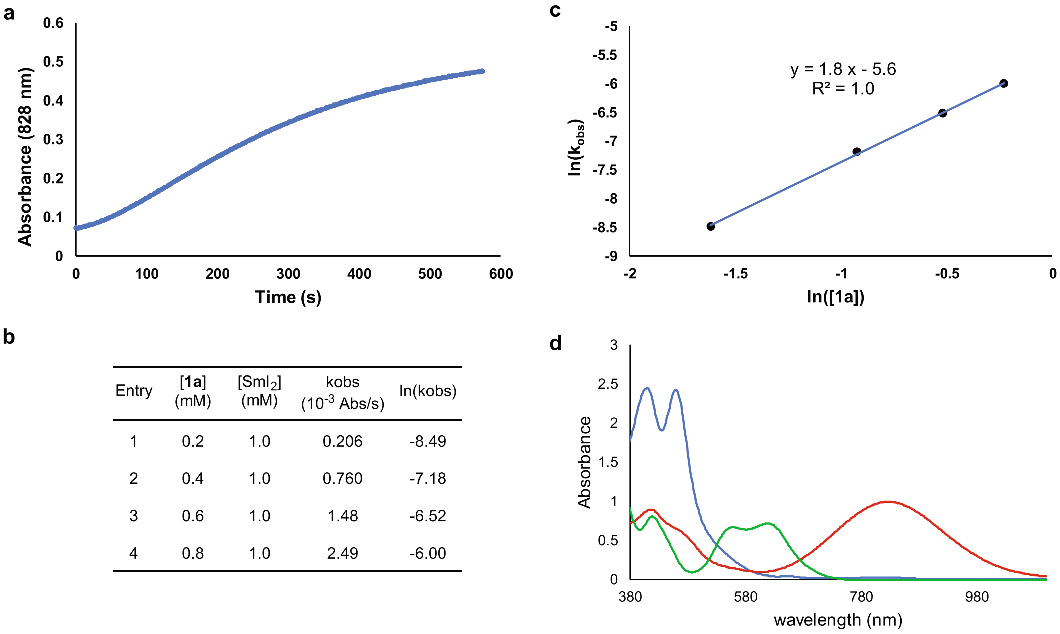

Entry	[**1a**] (mM)	[SmI_2] (mM)	kobs (10^{-3} Abs/s)	ln(kobs)
1	0.2	1.0	0.206	-8.49
2	0.4	1.0	0.760	-7.18
3	0.6	1.0	1.48	-6.52
4	0.8	1.0	2.49	-6.00

Extended Data Fig. 3 | Kinetic study of stoichiometric reactions. A kinetic study of the stoichiometric reaction was carried out by monitoring the formation of **4** by UV–vis spectroscopy at room temperature. A typical procedure is described below. A THF solution containing **1a** (1.2 μmol) was added into a quartz glass cell (1 cm × 1 cm × 4 cm) with a septum in a nitrogen-filled glove box. The THF solution of SmI_2 (3.0 μmol) was added to the quartz glass cell using a syringe with stirring. The total amount of solution was adjusted to be 3.0 ml. The spectra were measured every 0.4 s, and the rate was determined from the time profile of the initial 100 s. The reaction rate (k_{obs}, in abs s^{-1}) was determined from the formation rate of the absorbance of **4** at 828 nm. **a**, Typical time profile of the formation of **4** observed at 828 nm with SmI_2 (1.0 mM) and **1a** (0.4 mM) in THF at room temperature. **b**, Rate of formation of **4** at various concentrations of **1a**. **c**, Rate dependence of the formation of **4** on concentration of **1a** in THF. **d**, UV–vis absorption spectra between 380 and 1,100 nm of **1a** (0.48 mM in THF; blue line), **4** (0.60 mM in THF; red line), and SmI_2 (1.2 mM in THF; green line).

Extended Data Table 1 | Catalytic reactions with various molybdenum complexes as catalysts

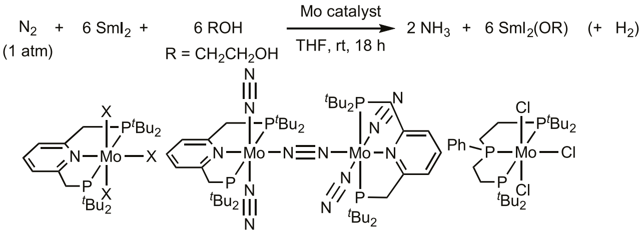

1b: X = Br
1c: X = Cl

2

3

Entry	Mo catalyst	NH_3 (equiv/Mo)	NH_3 (%)[a]	H_2 (equiv/Mo)	H_2 (%)[a]
1	**1b**	53.7±5.2[b]	89±6[b]	5.6±0.8[b]	6±2[b]
2	**1c**	52.1±0.0[b]	87±0[b]	6.9±1.0[b]	8±1[b]
3	**2**	28.2	44	31.5	34
4	**3**	9.3	19	56.9	62

$SmI_2(THF)_2$ was used as the source of SmI_2.

[a] Yield based on SmI_2.

[b] Data are mean of multiple individual experiments (at least 2) with error bars representing the s.d.

Extended Data Table 2 | Catalytic reactions in various solvents using typical experimental procedure

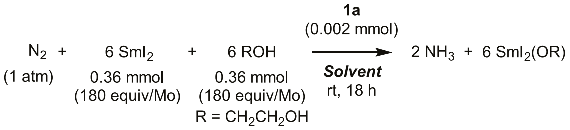

$$\underset{(1\ \text{atm})}{N_2} + \underset{\substack{0.36\ \text{mmol} \\ (180\ \text{equiv/Mo})}}{6\ SmI_2} + \underset{\substack{0.36\ \text{mmol} \\ (180\ \text{equiv/Mo}) \\ R = CH_2CH_2OH}}{6\ ROH} \xrightarrow[\substack{\textbf{\textit{Solvent}} \\ \text{rt, 18 h}}]{\substack{\mathbf{1a} \\ (0.002\ \text{mmol})}} 2\ NH_3 + 6\ SmI_2(OR)$$

Entry	***Solvent***	NH_3 (equiv/Mo)	NH_3 (%)[a]	H_2 (equiv/Mo)	H_2 (%)[a]
1	1,4-dioxane	2.1	3	49.0	53
2	MeCN	4.5	7	1.9	2
3	Et_2O	12.1	20	12.3	13
4	Toluene	7.8	13	13.0	14
5	Hexane	3.9	6	14.9	16
6	DMSO	0	0	0.7	1
7	$HOCH_2CH_2OH$	4.9	8	68.9	74
8	THF	42.8±1.5[b]	70±2[b]	22.2±4.5[b]	24±4[b]
9[c]	THF	0	0	71.7	78
10[d]	THF	–	0	–	4

$SmI_2(THF)_2$ was used as the source of SmI_2.

[a] Yield based on SmI_2.

[b] Data are mean of multiple individual experiments (at least 2) with error bars representing the s.d.

[c] The reaction was carried out under 1 atm of argon.

[d] The reaction was carried out in the absence of **1a**.

Extended Data Table 3 | Catalytic reactions using water as a proton source

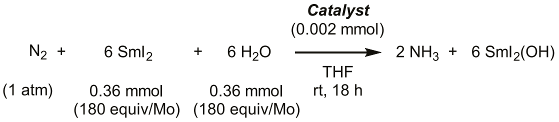

$$\underset{\text{(1 atm)}}{N_2} + \underset{\substack{\text{0.36 mmol}\\\text{(180 equiv/Mo)}}}{6\ SmI_2} + \underset{\substack{\text{0.36 mmol}\\\text{(180 equiv/Mo)}}}{6\ H_2O} \xrightarrow[\substack{\text{THF}\\\text{rt, 18 h}}]{\substack{\textbf{\textit{Catalyst}}\\\text{(0.002 mmol)}}} 2\ NH_3 + 6\ SmI_2(OH)$$

Entry	***Catalyst***	NH_3 (equiv/Mo)	NH_3 (%)[a]	H_2 (equiv/Mo)	H_2 (%)[a]
1	**1a**	26.8	43	36.0	39
2	**5**	39.4	67	9.4	11
3	**9**	57.3	95	1.2	1
4	none	-	0	-	2

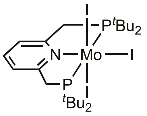

1a

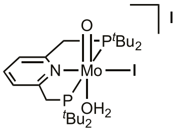

5

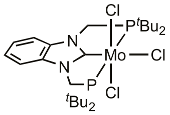

9

$SmI_2(THF)_2$ was used as the source of SmI_2.

[a] Yield based on SmI_2.

Extended Data Table 4 | Catalytic reactions using larger amounts of reducing reagent and proton source using 1a or 9 as catalysts

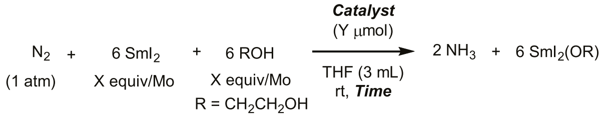

Entry	X (equiv/Mo)	Y (μmol)	*Time* (h)	NH_3 (equiv/Mo)	NH_3 (%)[a]	H_2 (equiv/Mo)	H_2 (%)[a]
1	7200	0.05 (**1a**)	18	300	13	1650	47
2	7200	0.05 (**9**)	18	1550±50[b]	67±9[b]	550±100[b]	15±6[b]
3	14400	0.025 (**9**)	20	3850	75	n.d.	n.d.
4	21600	0.025 (**9**)	48	3950	55	4600	43
5	28800	0.025 (**9**)	72	3500	34	n.d.	n.d.
6[c]	14400	0.025 (**9**)	4	3650±250[b]	76±6[b]	1600±150[b]	22±2[b]
7	21600	0.025 (**9**)	8	3600	50	n.d.	n.d.
8[d]	14400	0.025 (**9**)	4	4350±150[b]	91±4[b]	150±100[b]	2±1[b]

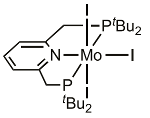

1a

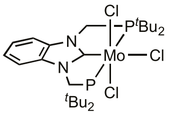

9

$SmI_2(THF)_2$ was used as the source of SmI_2.

[a] Yield based on SmI_2.

[b] Data are mean of multiple individual experiments (at least 2) with error bars representing the s.d.

[c] THF (2 ml) was used as a solvent.

[d] H_2O was used as a proton source.

n.d., not determined.

Extended Data Table 5 | Determination of the turnover frequencies of catalytic reactions

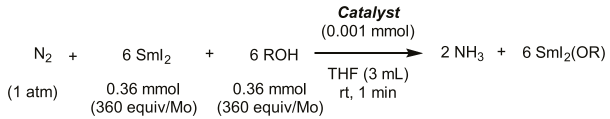

$$\underset{(1\ \text{atm})}{N_2} + \underset{\substack{0.36\ \text{mmol}\\(360\ \text{equiv/Mo})}}{6\ SmI_2} + \underset{\substack{0.36\ \text{mmol}\\(360\ \text{equiv/Mo})}}{6\ ROH} \xrightarrow[\substack{\text{THF (3 mL)}\\\text{rt, 1 min}}]{\substack{\textbf{\textit{Catalyst}}\\(0.001\ \text{mmol})}} 2\ NH_3 + 6\ SmI_2(OR)$$

Entry	***Catalyst***	ROH	NH_3 (equiv/Mo)	NH_3 (%)[a]	TOF (h^{-1})	TOF (min^{-1})
1	**1a**	$HOCH_2CH_2OH$	21.6	18	1300	21.6
2	**9**	$HOCH_2CH_2OH$	117.0	91	7000	117.0
3	**1a**	H_2O	7.3	6	400	7.3
4	**9**	H_2O	112.9	88	6800	112.9

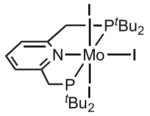

1a

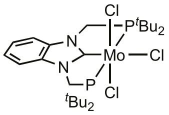

9

$SmI_2(THF)_2$ was used as the source of SmI_2.

[a] Yield based on SmI_2.

Extended Data Table 6 | Catalytic reduction by using hydrazine as a substrate instead of dinitrogen gas

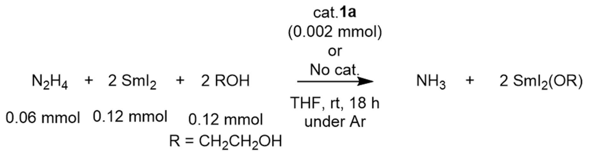

$$\underset{0.06\ \text{mmol}}{N_2H_4} + \underset{0.12\ \text{mmol}}{2\,SmI_2} + \underset{\substack{0.12\ \text{mmol}\\ R = CH_2CH_2OH}}{2\,ROH} \xrightarrow[\substack{\text{THF, rt, 18 h}\\ \text{under Ar}}]{\substack{\text{cat. }\mathbf{1a}\\ (0.002\ \text{mmol})\\ \text{or}\\ \text{No cat.}}} NH_3 + 2\,SmI_2(OR)$$

	NH_3	H_2	N_2H_4
1a (0.002 mmol)	83% yield based on N_2H_4	16% yield based on SmI_2	10% recovery based on N_2H_4
No cat.	36% yield based on N_2H_4	6% yield based on SmI_2	46% recovery based on N_2H_4